OUKA
The University of Osaka
Institutional Knowledge Archive

Title	MgO Effect on the Hydrothermal Solidification of Blast Furnace Slag
Author(s)	Yoshikawa, Takeshi; Hosokawa, Masaru; Tanaka, Toshihiro
Citation	ISIJ International. 2008, 48(5), p. 557-562
Version Type	VoR
URL	https://hdl.handle.net/11094/26388
rights	© 2008 ISIJ
Note	

The University of Osaka Institutional Knowledge Archive : OUKA

https://ir.library.osaka-u.ac.jp/

The University of Osaka

ISIJ International, Vol. 48 (2008), No. 5, pp. 557–562

MgO Effect on Hydrothermal Solidification of Blast Furnace Slag

Takeshi YOSHIKAWA, Masaru HOSOKAWA and Toshihiro TANAKA

Division of Materials and Manufacturing Science, Graduate School of Engineering, Osaka University, Suita, Osaka 565-0871 Japan.

(*Received on January 9, 2008; accepted on February 26, 2008*)

Due to the large generation of blast furnace (BF) slag, new recycling processes that produce valuable materials are required. The authors have focused on a hydrothermal treatment of BF slag using waste heat exhausted from iron- and steelmaking processes. Although BF slag contains Al_2O_3, which is well known to have a deteriorating effect on hydrothermal reactions, especially CaO–SiO_2 hydration, it can be successfully solidified by hydrothermal treatment above 523 K. We focused on the contribution of MgO in BF slag to the hydrothermal reactivity in the slag system. The hydrothermal solidification of synthesized CaO–SiO_2–Al_2O_3 and CaO–SiO_2–Al_2O_3–MgO slags were investigated in the present work. The hydrothermal solidification behaviors of slags are discussed based on the degree and type of crystal formation during the hydrothermal process.

KEY WORDS: blast furnace slag; hydrothermal reaction; hydrothermal hot pressing; flexural strength.

1. Introduction

Blast furnace (BF) slag is the greatest by-product in iron- and steelmaking processes, the generation of which amounted to 24.8 billion tones in Japan during 2006.[1] Although most BF slag is recycled for raw materials of roadbed, cements and concrete aggregates, new processes for producing more valuable materials are demanded. Since this slag consists of major components of ceramic materials such as SiO_2, CaO, Al_2O_3 and MgO, high temperature treatments based on melting or sintering are generally applied for conversion into functional ceramics. When the energy consumption and CO_2 emission are considered, however, such high temperature processes may not be feasible for recycling. Therefore, the authors have focused on the application of hydrothermal reactions to the slag. At the hydrothermal condition, the materials are exposed to highly reactive water with a high pressure water vapor and/or a high temperature aqueous solution. The reaction takes place at a temperature ranging from 423 to 623 K, which can be controlled using waste heat exhausted from the iron- and steelmaking processes. Hydrothermal treatments of BF slag have been applied for productions of a heat storage material and a high strength building material with some additives.[2–4] In addition, the authors have applied the hydrothermal reaction to glass and BF slag for conversion into functional materials by introducing water into the original materials.[5–8]

The CaO–SiO_2–Al_2O_3 system is generally used for manufacturing a functional calcium silicate board by hydrothermal treatment below 473 K. The board is mainly produced from cement and quartz sand. The product exhibits excellent properties in heat-insulation and lightness as well as physical strength because vigorous needle-shaped crystals of tobermorite (calcium silicate hydrate; $5CaO \cdot 6SiO_2 \cdot 5H_2O$) formed after the hydrothermal reaction combine the original constitutional particles. However, as source materials containing a large Al_2O_3 content are not usually used because of the deteriorating effect of Al_2O_3 on the hydrothermal reaction,[9,10] BF slag that contains 15–20 mass% Al_2O_3 has not been used in calcium silicate material production. On the other hand, recent researches[3,4,6,7] revealed BF slag can be hydrothermally solidified in spite of containing Al_2O_3. Especially, water-cooled BF slag mainly possessing glass structure was found to solidify strongly compared with air-cooled BF slag of mostly crystalline structure.[5] Hence, we focused on the effect of the minor component of MgO on the hydrothermal solidification of water-cooled BF slag, which may modify the deterioration by Al_2O_3 in the hydrothermal reaction of BF slag.

To understand the hydrothermal solidification of BF slag, solidification behavior of the CaO–SiO_2–Al_2O_3 system and the effect of MgO were investigated in the present work. Slags were subjected to the hydrothermal treatments using the hydrothermal hot pressing technique[11] at 573 K. Solidified materials were characterized by X-ray diffraction analysis and flexural strength measurements. The effect of MgO on the solidification behavior of CaO–SiO_2–Al_2O_3 is discussed for the crystal formation during the hydrothermal reaction.

© 2008 ISIJ

2. Experimental

2.1. Materials

The chemical composition of the water-cooled BF slag used is shown in **Table 1**. Synthesized $CaO–SiO_2–Al_2O_3$ and $CaO–SiO_2–Al_2O_3–MgO$ slag samples were prepared from reagent grade quartz and $CaCO_3$, Al_2O_3 and MgO powders. Twenty grams of mixture of these powders were melted in a Pt–20%Rh crucible at 1 873 K for 3 h in air, which was followed by rapid cooling on a copper block. BF slag and synthesized slags were confirmed to be of glass structure by X-ray diffraction analysis.

2.2. Hydrothermal Hot Pressing of Slag Powder

BF slag and synthesized $CaO–SiO_2–Al_2O_3(–MgO)$ slags were subjected to the hydrothermal hot pressing (HHP) method developed by Yamasaki *et al.*[11] Details of the apparatus are given in our previous work.[8] Each slag was ground and sieved at 180 μm, and mixed with purified water at a mass ratio of slag : water of 10 : 3. The mixture was charged in an HHP autoclave with an internal diameter of 20 mm. After the mixture was pressed at 40 MPa, the autoclave was heated to 573 K within 20 min and held for a predetermined time. Cooling was achieved to room temperature within 20 min. Obtained compacts were examined by X-ray diffraction (XRD) analysis as well as flexural strength measurement to evaluate the degree of solidification.

2.3. Flexural Strength Measurement of HHP Treated Slag Compact

The slag compact with a diameter of 20 mm prepared after hydrothermal hot pressing at 573 K for 1 h was adjusted to be almost 5 mm in thickness by polishing with #3000 emery paper. The compact was subjected to a three point bending test. After the compact was placed in the sample holder illustrated in **Fig. 1**, it was set in a universal testing machine (Autograph AG-1 100 kN, Shimadzu Corp.). Load tests were operated at a loading speed of 0.1 mm/min. The flexural strength, σ_f (Pa), is determined by the following equation.

$$\sigma_f = \frac{3PL}{2wt^2} \quad \text{.....(1)}$$

Here, P (N), L (m) and t (m) are the maximum load at a fracture point, the length between the support spans (8.0×10^{-3} m) and the thickness of the specimen, respectively. The width of the disk specimen, w (m), is assumed to be its diameter, in view of the short span length. Stainless steel pins for supports and loading point had a diameter of 4 mm. Measurements were performed four and three times for BF slag and synthesized slag, respectively.

Table 1. Chemical composition of water-cooled BF slag (mass%).

SiO_2	CaO	Al_2O_3	MgO	MnO	T.Fe	S
35.8	41.5	15.3	5.48	0.28	1.58	0.79

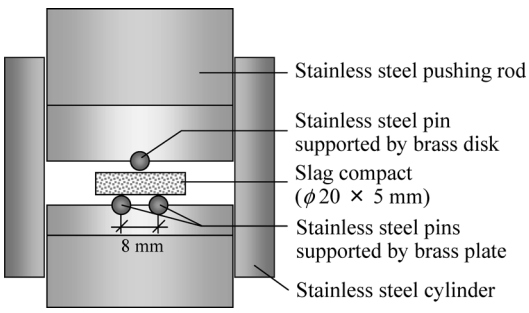

Fig. 1. Schematic diagram of a workpiece for the flexural strength measurement of slag compact.

3. Results and Discussions

3.1. Hydrothermal Solidification of BF Slag and Synthesized $CaO–SiO_2–Al_2O_3(–MgO)$ Slag

The water-cooled BF slag powder was well solidified after the hydrothermal hot pressing at 573 K for 1 h. The apparent density of the obtained compact was determined to be about 2.0 g/cm^3 by measuring its thickness. **Figure 2** shows a XRD pattern for the hydrothermally treated BF slag. Although the major phase is regarded to be of glass structure, hibschite (calcium aluminum silicate hydroxide; $Ca_3Al_2Si_2O_8(OH)_4$) is identified as the only crystalline phase. Hibschite is considered to work for the hydrothermal solidification of BF slag because it is well known that hydrate or hydroxide crystals formed after the hydrothermal process strongly combine the constitutional particles in the resulting materials. To understand the morphological change by the hydrothermal reaction of BF slag, the HHP-treated sample was subjected to scanning electron microscopy. The microstructure is shown in **Fig. 3**. The hydrothermally reacted phase fills the intragrain space of slag

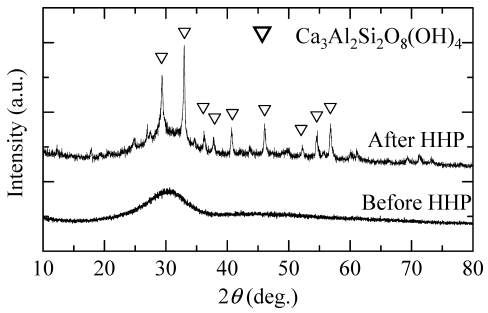

Fig. 2. XRD patterns for BF slags before and after the hydrothermal hot pressing at 573 K for 1 h.

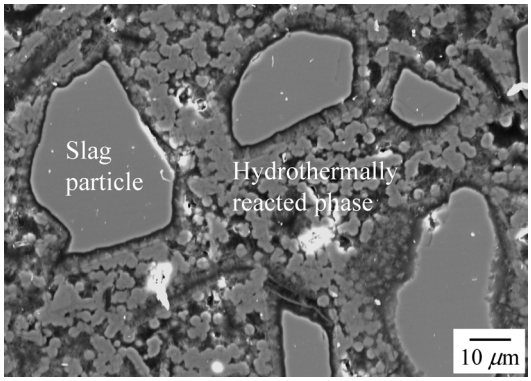

Fig. 3. Microstructure of BF slag compact after the hydrothermal hot pressing at 573 K for 1 h.

© 2008 ISIJ

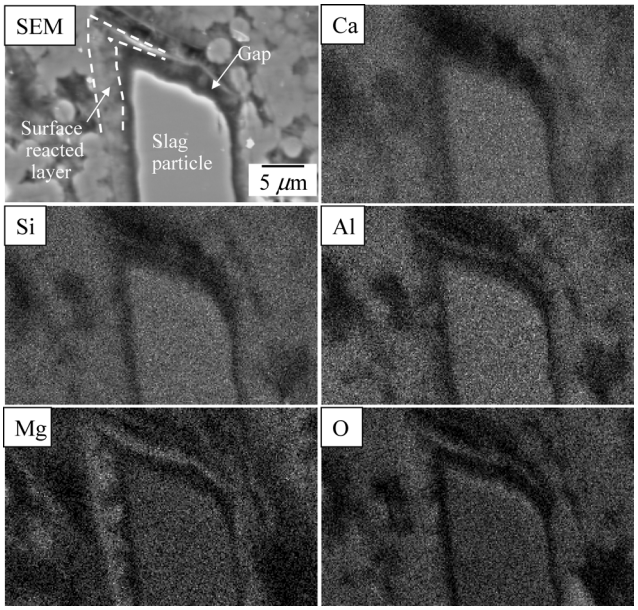

Fig. 4. Element distributions around the slag particle after the hydrothermal hot pressing at 573 K for 1 h.

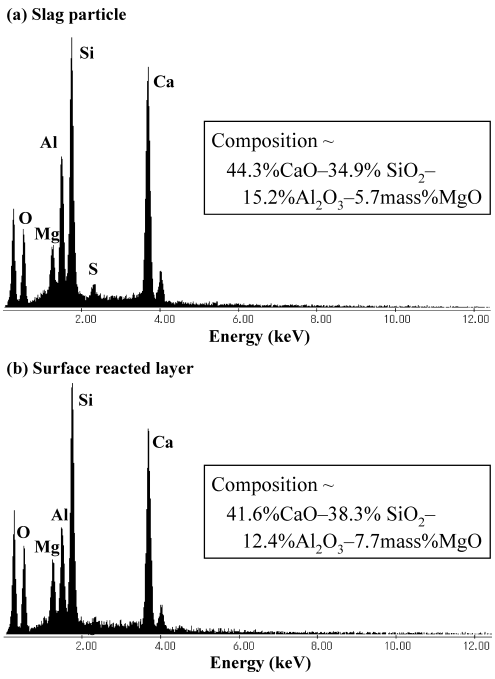

Fig. 5. EDX profiles at (a) internal portion and (b) surface reacted layer of the slag particle in Fig. 4.

particles. Focusing on the surface of a slag particle as shown in **Fig. 4**, a dark-colored layer 1–3 μm in thickness is observed. Electron dispersive X-ray analysis for spatial distribution of elements in Fig. 4 and for quantitative local analysis as shown in **Fig. 5** revealed; magnesium is concentrated in the surface layer and calcium and aluminum are diluted compared with the distributions in the unreacted inner portion of the slag particle. This suggests magnesium contributes to the formation of the layer. As no significant phase except for hibschite was observed in the XRD analysis, the layered phase is considered to be the hydrated glass formed after dissolution of water into original slag particles. It is speculated that the formation of the hydrated glass layer results in faster mass transfers of the components to the slag surface and larger crystallizations. Details are discussed in our other work.[12] In Fig. 4, a gap can be observed between the surface reacted layer and the inner particle, which might be formed after the defoliation of the reacted layer during polishing due to its brittle structure.

Table 2. Conditions for the hydrothermal hot pressing of the synthesized $CaO–SiO_2–Al_2O_3$ and $CaO–SiO_2–Al_2O_3–MgO$ slags.

Slag No.	Slag composition (mass%) SiO_2	CaO	Al_2O_3	MgO	Time (min)	Solidification
A	70	20	10			×
B	60	30	10		60	×
C	55	35	10			○
D	50	40	10		30	×
					60	○
					180	○
E	45	45	10			○
F	40	50	10			○
G	55	30	15			×
H	50	35	15	0		×
I	45	40	15			○
J	40	45	15			○
K	70	10	20		60	×
L	60	20	20			×
M	50	30	20			×
N	40	40	20			×
O	40	30	30			×
P	30	30	40			×
Q	10	50	40		10	○
					30	○
					60	○
A2	67.7	19.3	9.7	3.3		×
B2	58.0	29.0	9.7	3.3	60	×
C2	53.2	33.8	9.7	3.4		○
D2	49.7	39.7	9.9	0.7	30	○
D3	48.3	38.6	9.7	3.4	30	○
					60	
E2	43.5	43.5	9.7	3.4	30	○
					60	
F2	38.6	48.3	9.7	3.4		○
G2	53.2	29.0	14.5	3.3	60	×
H2	48.4	33.8	14.5	3.3		○
I2	43.5	38.7	14.5	3.3	30	○
					60	
J2	39.7	44.7	14.9	0.7		○
J3	39.3	44.3	14.8	1.6		○
J4	38.7	43.5	14.5	3.3		○
J5	38.0	42.7	14.3	5.0		○
J6	37.3	42.0	14.0	6.7		○
K2	67.8	9.7	19.4	3.2	60	×
L2	58.1	19.4	19.4	3.2		×
M2	48.4	29.0	19.4	3.2		×
N2	38.7	38.7	19.4	3.2		×
O2	38.8	29.1	29.1	3.1		×
P2	29.0	29.0	39.0	3.0		×
Q2	9.7	48.5	38.8	3.0	30	○

Experimental conditions for the hydrothermal hot pressing of the synthesized $CaO–SiO_2–Al_2O_3$ and $CaO–SiO_2–Al_2O_3–MgO$ slags are summarized in **Table 2**. Compositions of the HHP treated samples of the $CaO–SiO_2–Al_2O_3$ ternary slag are represented by alphabetic letters in **Fig. 6**. The solidification was achieved after the hydrothermal hot pressing at 573 K for 1 h for the compositions denoted with the circled alphabetic letters. Concerning the hydration in the $CaO–SiO_2$ based system for the production of cement and calcium silicate building materials, a molar ratio of $CaO/SiO_2=0.83$ is recognized to be favored for hydrother-

© 2008 ISIJ

mal solidification.[13,14] This ratio is in accordance with that of tobermorite ($5CaO \cdot 6SiO_2 \cdot 5H_2O$), which is well known to be a key product phase working as a binder in the calcium silicate materials. The composition of tobermorite is projected on the phase relation for the $CaO–SiO_2–Al_2O_3$ system by a double circle in Fig. 6. Slags of which compositions are located around the tobermorite composition were well solidified, and deviation from the tobermorite composition leads to less solidification. At 20 mass% Al_2O_3, slags were not solidified. This suggests a deteriorating effect by Al_2O_3 on the hydrothermal solidification in the $CaO–SiO_2–Al_2O_3$ system as reported previously.[9,10] On the other hand, slag Q was strongly solidified even with a hydrothermal reaction for 10 min. In addition, this slag started to agglutinate during mixing with purified water at room temperature, which indicates its high reactivity with water.

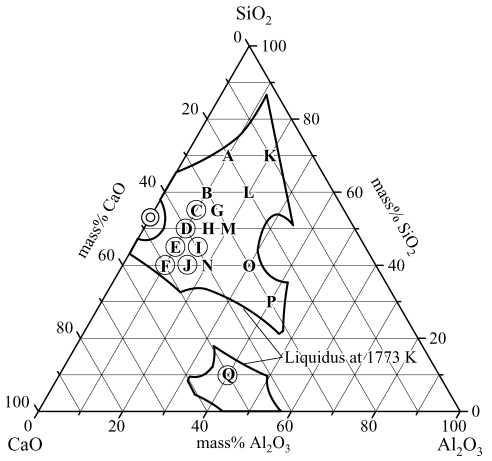

Fig. 6. Slag composition in the $CaO–SiO_2–Al_2O_3$ system subjected to the hydrothermal treatment. Encircled letters correspond to compositions where solidification occurs after the hydrothermal hot pressing at 573 K for 1 h.

The effect of MgO on the hydrothermal solidification of the $CaO–SiO_2–Al_2O_3$ slag can be discussed by looking at Table 2. MgO is added at almost 3 mass% to the $CaO–SiO_2–Al_2O_3$ slag except for slags D and J. Although slags D and H were not solidified within 30 and 60 min in the $CaO–SiO_2–Al_2O_3$ ternary system, the solidification of the $CaO–SiO_2–Al_2O_3–MgO$ quaternary slag was achieved in the identical hydrothermal condition (slags D3 and H2). Especially, addition of 0.7 mass% MgO (slag D2) was ef-

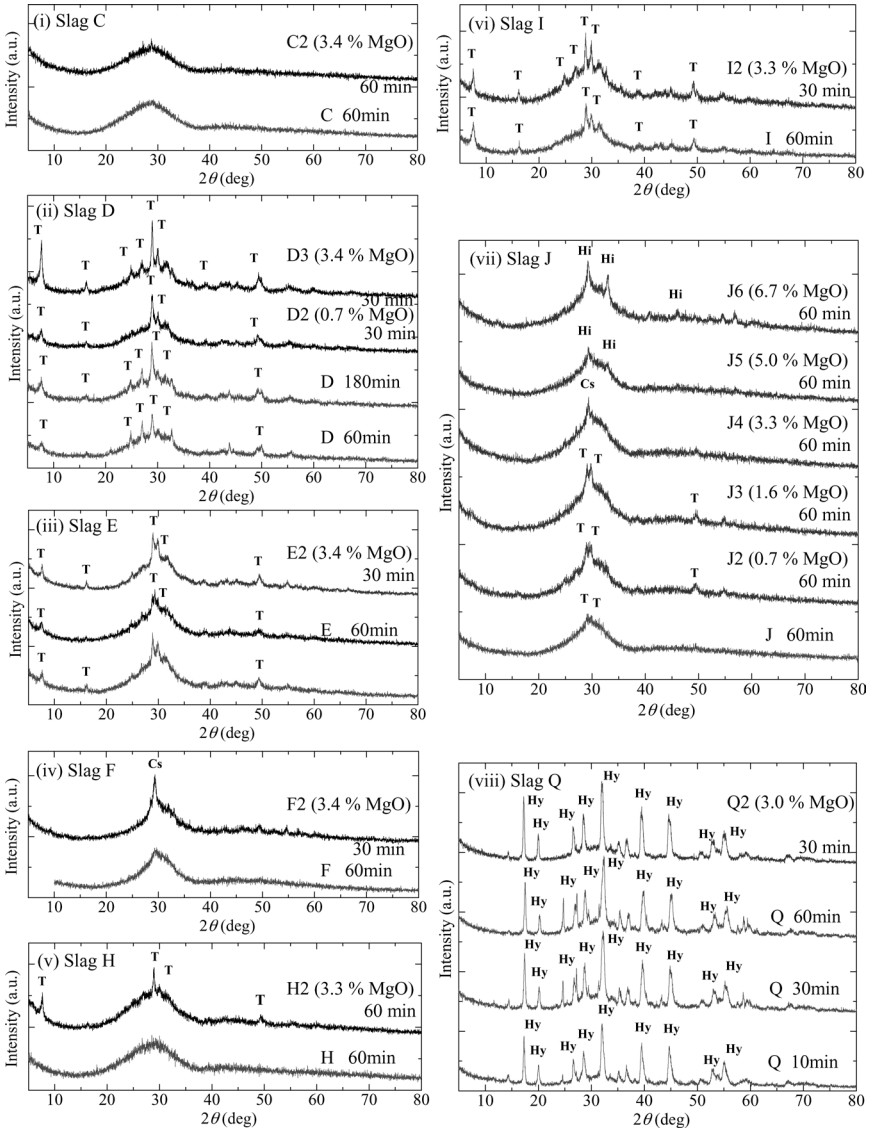

Fig. 7. XRD patterns for the HHP-treated $CaO–SiO_2–Al_2O_3$ and $CaO–SiO_2–Al_2O_3–MgO$ slags. Crystalline phases; T: tobermorite, Cs: Calcium silicate hydrate, Hi: hibschite, Hy: hydrogarnet

© 2008 ISIJ

fective in the solidification of slag D.

To understand the hydrothermal reaction of CaO–SiO_2–Al_2O_3 and CaO–SiO_2–Al_2O_3–MgO slags, XRD analysis was carried out on the HHP-treated materials. **Figure 7** shows the XRD patterns for the solidified slags. Except for slag Q, the resulting materials are mainly composed of the glass phase. In the slags D, E and I, tobermorite is identified in the ternary system, and its formation was increased by MgO addition to the corresponding slags. In particular, addition of even 0.7 mass% MgO to slag D (slag D2) resulted in the rapid formation of tobermorite, which is shown by the comparable peak intensities for slag D after a treatment for 180 min and for D2 after 30 min. Although ternary slags C and H apparently do not contain a crystalline phase, slight crystallization (slag C2) and tobermorite formation (slag H2) are observed in MgO-added quaternary slags, respectively. Slag F is also accelerated to crystallize by MgO addition with the appearing phase being low-crystalline calcium-silicate hydrate ($xCaO \cdot SiO_2 \cdot zH_2O$). Concerning slag J, the effect of MgO on the crystal formation after the hydrothermal reaction was investigated for various amounts of added MgO. The composition of this slag is closely related to the mass ratio of the three major components of CaO, SiO_2 and Al_2O_3 in BF slag. Figure 7 (vii) shows an XRD pattern of slag J together with those of 0.7–6.7 mass% MgO added quaternary slags. Without MgO addition (slag J), the observed crystalline phase is tobermorite, and its formation increases with MgO addition up to a content of 1.6 mass%. When MgO is added by 3.3 mass%, the appearing crystalline phase in the HHP sample is low-crystalline calcium-silicate hydrate. With more than 5.0 mass% MgO, hibschite is formed as observed in BF slag. Since the MgO content of BF slag is as much as 5.48 mass%, hibschite formation in BF slag after the hydrothermal treatment is regarded to be controlled by dissolved MgO. On the other hand, no apparent peaks were observed in unsolidified materials after the hydrothermal hot pressing. Henceforth, it is suggested crystal formation is an essential process in the hydrothermal solidification of slags, and MgO in BF slag contributes significantly to solidification and controls the resulting crystalline phase during the hydrothermal reaction.

In the series for slag Q, the formation of hydrogarnet (calcium aluminate hydrate; $Ca_3Al_2(OH)_{12}$) is clearly observed. Its formation is recognized to be a dominant reaction in the early stage of hydration of the CaO–SiO_2 materials containing high Al_2O_3 content[15] and may work for the rapid solidification mentioned above.

3.2. Flexural Strength of Hydrothermally Treated BF Slag and Synthesized CaO–SiO_2–Al_2O_3(–MgO) Slag

A flexural strength measurement was conducted for solidified compacts of BF slag and synthesized CaO–SiO_2–Al_2O_3 slags C–F and I–J. In addition, the effect of MgO on the physical property of the slag compact was investigated by adding almost 3 mass% MgO to above synthesized slags and measuring the flexural strengths. The flexural strengths are summarized in **Fig. 8** together with the crystalline phase identified by XRD analysis. The flexural strength of solidified BF slag ranges from 11 to 23 MPa. Its average value of 16 MPa is larger than the required value of 4.5 MPa for ready-mix concretes.[16] Hence, building materials can possibly be produced by a hydrothermal reaction with BF slag as the only starting material.

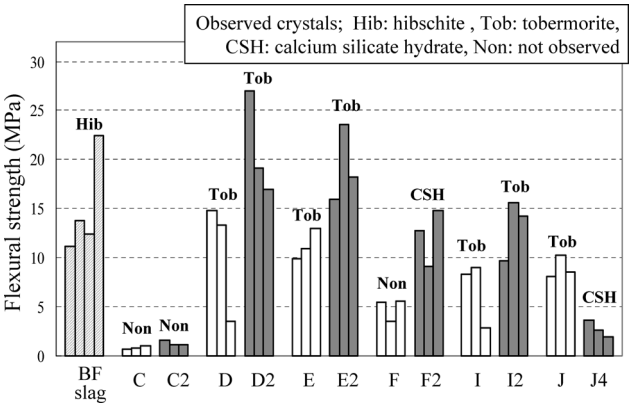

Fig. 8. Measured flexural strength of the HHP compact of BF slag and synthesized CaO–SiO_2–Al_2O_3(–MgO) slag.

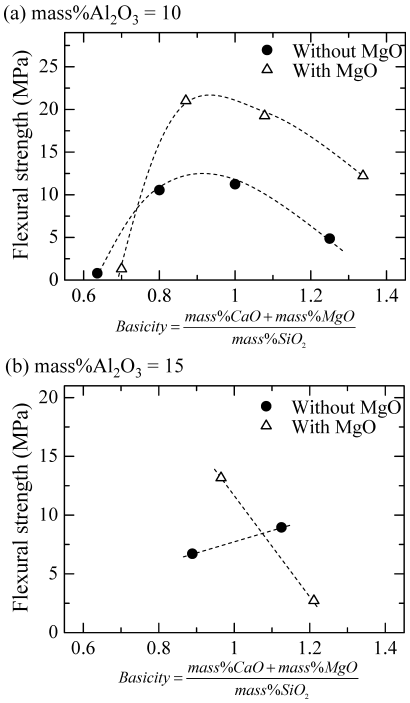

Fig. 9. Flexural strength of the solidified slag compact against slag basicity for an iso-content of Al_2O_3.

For the synthesized slags, slags D and E with compositions close to that of tobermorite exhibit higher flexural strengths than do slags of other compositions. The determined physical property relates strongly to the degree of crystallization during the formation of identical crystals. Except for slag J, the flexural strengths of solidified materials increase with MgO addition. To understand the MgO effect on the hydrothermal solidification of the CaO–SiO_2–Al_2O_3 slag, the flexural strengths are arranged against slag basicity in **Fig. 9** at constant Al_2O_3 contents, where each value of the flexural strength is derived from the average of the three measurements. Here, the slag basicity is defined to be (mass%CaO+mass%MgO)/mass%SiO_2, assuming comparable contributions of CaO and MgO to the slag basicity. When Al_2O_3 content is

© 2008 ISIJ

10 mass%, the strengths are clearly divided into MgO-free and MgO-added groups and possess peak (mass%CaO+mass%MgO)/mass%SiO_2∼1. The flexural strength is doubled by MgO addition, which indicates the MgO effect on the hydrothermal solidification is far beyond its contribution to the slag basicity. At 15 mass% Al_2O_3, however, the MgO effect is not obvious. Especially at (mass%CaO+mass%MgO)/mass%SiO_2=1.1–1.2, corresponding to slag J in Table 2, the flexural strength is decreased by MgO addition. This is related to the formed crystal which is tobermorite for MgO-free slag and low-crystalline calcium silicate hydrate for MgO added slag. Tobermorite is the most well-known crystal for hardening hydrothermally treated materials, and is considered to bring larger flexural strength to the ternary slag. Furthermore, the fact that BF slag solidifies much more strongly than does the slag J4 in spite of similar matrix composition suggests a larger contribution to the solidification by hibschite than by low-crystalline calcium silicate hydrate.

Accordingly, it was found the physical property of the hydrothermally solidified material in the CaO–SiO_2–Al_2O_3 system is improved by MgO addition during the formation of identical crystals. This is due to the contribution of MgO to the rapid crystal formation during the hydrothermal treatment. Although BF slag has been expected to be less solidified with hydrothermal treatment due to the Al_2O_3 effect, MgO contained in the slag modifies its reactivity and gives sufficient physical property of the solidified compact.

4. Conclusions

To understand hydrothermal solidification of BF slag, the hydrothermal hot pressing method was conducted on BF slag and CaO–SiO_2–Al_2O_3(–MgO) slag at 573 K under a compression at 40 MPa. The solidified materials were examined by XRD analysis and flexural strength measurement. The results obtained are as follows.

(1) Hydrothermal solidification in the CaO–SiO_2–Al_2O_3 system was obtained around the composition of tobermorite. MgO addition to the ternary slag resulted in the faster solidification.

(2) From XRD analysis of the hydrothermally treated slags, the crystal formation during the hydrothermal reaction was found to be the significant process for hydrothermal solidification. With the addition of MgO to the CaO–SiO_2–Al_2O_3 slag, crystallization was accelerated.

(3) Flexural strengths of the HHP treated slag compacts increased with increasing crystallization. When MgO was added to the CaO–SiO_2–Al_2O_3 slag as 3 mass%, the flexural strength doubled. Hence, it was found that MgO contributed for the hydrothermal solidification by accelerating the crystal formation during the hydrothermal reaction.

Acknowledgement

This research is partly supported by a Research Promotion Grant from the Iron and Steel Institute of Japan and Priority Assistance for the Formation of Worldwide Renowned Centers of Research—The Global COE Program (project: Center of Excellence for Advanced Structural and Functional Materials Design) from the Ministry of Education, Culture, Sports, Science and Technology (MEXT), Japan. The authors are thankful to Prof. Utsunomiya for his help with the flexural strength measurement of the slag compact.

REFERENCES

1) http://slg.jp/tokei/japan/18/index2.htm.
2) Y. Sugano, R. Sahara, T. Murakami, T. Narushima, Y. Iguchi and C. Ouchi: *ISIJ Int.*, **45** (2005), 937.
3) Z. Jing, E. H. Ishida, F. Jin, T. Hashida and N. Yamasaki: *Ind. Eng. Chem. Res.*, **45** (2006), 7470.
4) Z. Jing, F. Jin, T. Hashida, N. Yamasaki and E. H. Ishida: *J. Mater. Sci.*, **42** (2007), 8236.
5) S. Maeda, N. Hirai, S. Katsuyama and T. Tanaka: *CAMP-ISIJ*, **18** (2005), 239.
6) M. Nakamoto, J. Lee, T. Tanaka, J. Ikeda and S. Inagaki: *ISIJ Int.*, **45** (2005), 1567.
7) S. Sato, T. Yoshikawa and T. Tanaka: *ISIJ Int.*, **47** (2007), 245.
8) T. Yoshikawa, S. Sato and T. Tanaka: *ISIJ Int.*, **47** (2007), 130.
9) I. Stebnicka-Kalicka: *Therm. Anal.*, **1** (1980), 369.
10) K. Takemoto: *J. Ceram. Soc. Jpn.*, **73** (1965), C91.
11) N. Yamazaki, K. Yanagisawa, M. Nishioka and S. Kanahara: *J. Mater. Sci. Lett.*, **5** (1986), 355.
12) T. Yoshikawa, M. Hosokawa and T. Tanaka: *CAMP-ISIJ*, **20** (2007), 235.
13) S. A. Hamid: *Zeit. Krist.*, **154** (1981), 189.
14) Z. Jing, N. Matsuoka, F. Jin, N. Yamasaki, K. Suzuki and T. Hashida: *J. Mater. Sci.*, **41** (2006), 1579.
15) D. S. Klimesh and A. Ray: *Cem. Concr. Res.*, **28** (1998), 1109.
16) Ready-mixed concrete, JIS A5308, (2003), Japanese Industrial Standards Committee, Tokyo, Japan.

© 2008 ISIJ